Evaluation of chlorine decay models under transient conditions in a water distribution system

Hyunjun Kim and Sanghyun Kim

ABSTRACT

Residual chlorine concentration decreases along distribution networks because of factors such as water quality, physical properties of the pipeline, and hydraulic conditions. Hydraulic conditions are primarily governed by transient events generated by valve modulation or pumping action. We investigate the impact of transient events on the rate of chlorine decay under various flow conditions. To comprehensively compare the performance of existing chlorine models, 14 candidate models for chlorine concentration were used under various transient conditions. Two-dimensional (2D) transient flow analysis was conducted to investigate the unknown processes of chlorine decay under transient conditions. General formulations for modeling chlorine decay were used to comprehensively study the decay under unsteady conditions and to effectively incorporate the impact of transients into generic model structures. The chlorine decay patterns in the constructed water distribution system were analyzed in the context of transient events. Linear relationships between the model parameters and the frequency of transient events were determined under unsteady conditions, and the impact of turbulence intensity was successfully incorporated into model parameter evaluations. The modeling results from 2D transient analysis exhibit similar predictability as those obtained from calibration using the genetic algorithm.

Key words | chlorine concentration, modeling, unsteady conditions, water distribution systems

Hyunjun Kim
Sanghyun Kim (corresponding author)
Department of Environmental Engineering,
College of Engineering, Pusan National University,
Busandaekak-ro 63 beon-gil, Geumjeong-gu,
Busan 609-735,
Republic of Korea
E-mail: *kimsangh@pusan.ac.kr*

INTRODUCTION

Drinking water obtained from water treatment plants is disinfected before it enters a distribution system. Chlorine is the most widely used disinfectant to prevent the regrowth of microbial pathogens in treated water (Termini & Viviani 2015). Therefore, maintaining sufficient chlorine concentration throughout the water distribution system is an important aspect of water quality management. However, the concentration of residual chlorine in a water transmission system varies with system properties (Mohapatra *et al.* 2014).

The decay of chlorine is influenced by two distinct pathways. The first involves water quality parameters such as the concentration of organics, initial concentration of chlorine, iron content, rechlorination, and temperature, (Jadas-Hecart *et al.* 1992; Kiene *et al.* 1998; Powell 1998; Hua *et al.* 1999, 2015; Hallam *et al.* 2003; Vieira *et al.* 2004; Warton *et al.* 2006; Courtis *et al.* 2009), and the second involves system parameters such as pipe age, materials, and hydraulic conditions (LeChevalier 1990; Menaia *et al.* 2002; Li *et al.* 2003; Ramos *et al.* 2010; Al-Jasser 2011, 2007; Abokofa *et al.* 2016). Several studies have investigated the role of hydraulics in chlorine decay. A first-order decay model and its modifications have been widely used to predict chlorine decay in water distribution systems (Qualls & Johnson 1983; Haas & Karra 1984;

doi: 10.2166/hydro.2017.082

Jadas-Hecart *et al.* 1992; Meng *et al.* 2013). Menaia *et al.* (2002) investigated the relationship between flow velocity and first-order decay rate. Kim *et al.* (2015a) delineated a strong relationship between the Reynolds number (Re) and decay coefficient for a generalized chlorine prediction model.

The majority of experimental studies on chlorine decay have been conducted under conditions of constant pressure and velocity. A strong relationship between wall decay kinetics and flow characteristics (pipe diameter and flow velocity) also indicated the importance of hydraulics in chlorine residual (Termini & Viviani 2015). A large number of chlorine models for water distribution systems used flow rate and flow direction for prediction and calibration of unknown parameters (EPA 2005). Treated water flowing through a transmission system can also be investigated under unsteady flow conditions (Hoskins & Stoianov 2014; Rezaei *et al.* 2015). Li *et al.* (2003) evaluated the concentrations of residual chlorine for various retention times in a water distribution system. The advection reaction equation under water-hammer conditions was modeled by Fernandes & Karney (2004). A self-adaptive hydraulic and chlorine decay model was developed, and the relationship between chlorine decay rate and shear stress was shown, but precise mechanisms for chlorine decay under unsteady hydraulic conditions have not been explained completely (Aisopou *et al.* 2014). Ramos *et al.* (2010) reported, with limited experimental results, that a transient flow event could attenuate the decay of residual chlorine owing to a decrease in Reynolds number induced by rapid valve closure. Preliminary experimental results for chlorine decay for three different frequencies of transient events have been reported (Kim *et al.* 2015b). However, a comprehensive understanding of the relationship between transient flow events and chlorine decay, and the underlying processes, has not yet been achieved.

The purpose of this study is to compare the performance of existing chlorine models, to further the understanding of the impact of transient flow events on chlorine decay, and to implement the transient impact for chlorine modeling in water distribution systems. Ultimately, this study aims to develop a generic model to evaluate residual chlorine concentrations under unsteady flow conditions. For this purpose, the following objectives were explored. First, the variation in residual chlorine concentration under various unsteady flow conditions was monitored using a pilot-scale water distribution system. A transient generator was installed into a pipeline system to generate and regulate transient events. Second, the performances of the comprehensive models for chlorine decay were evaluated under unsteady conditions. A genetic algorithm (GA) was integrated into these models, and the parameters were calibrated to minimize the root-mean-square errors (RMSEs) between the observed and simulated chlorine concentrations. To generalize the existing models, the ranges of the orders for the *n*th- and limited *n*th-order models for chlorine decay were extended to include all real numbers, and the concentration of the stable component parameter was calibrated to address the effects of transient events on the reaction rates of chlorine compounds. Third, two-dimensional (2D) analysis of transient flow was conducted to quantify and characterize the impact of transients on the intensity of turbulence. Finally, generic equations for chlorine decay under transient conditions were developed and implemented into the models.

MATERIALS AND METHODS

Experimental setup

A pilot-scale water distribution system was designed and used to evaluate temporal variations in residual chlorine concentrations under a wide range of flow conditions. The pipeline was 125 m in length, with one pressurized tank, one reservoir tank, and a serial pump system with three pumps (Figure 1). The pipe was made of stainless steel with an elastic modulus of 190 GPa. The inner diameter and thickness of the pipe were 0.02 m and 0.003 m, respectively. The pressurized tank was connected to the discharge of the serial pump system, and it provided sufficient pressure head for stable water circulation at a designated velocity throughout the system. The reservoir tank was connected at the downstream end of the pipe. The serial pump system was installed between the two tanks to generate various hydraulic conditions ranging between Reynolds numbers (Re) of 2,000 and 800,000. In this study, the Re

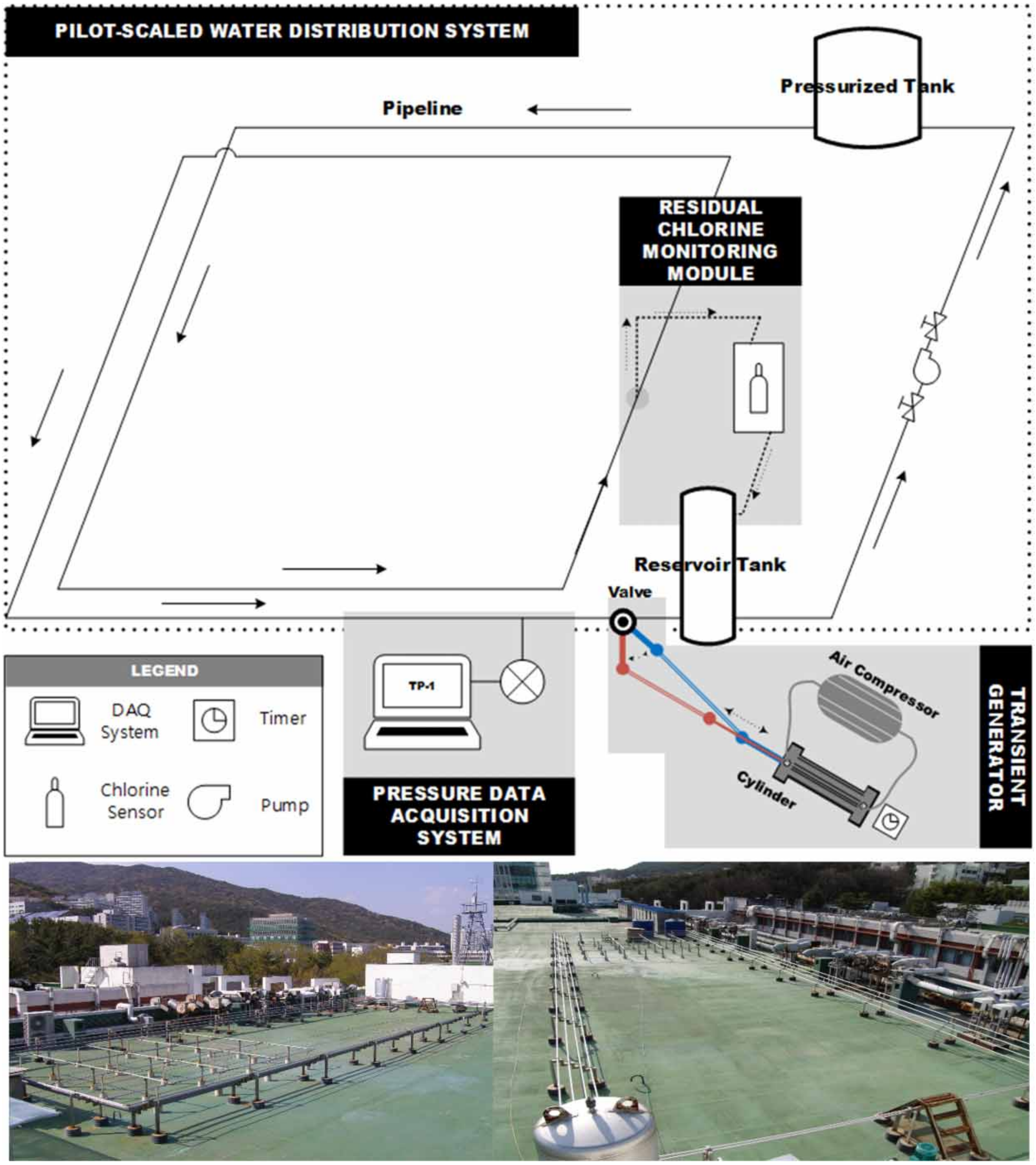

Figure 1 | A schematic and photographs of an experimental pipeline system with a transient generator.

for a steady flow condition was 140,000. The measurement range of the chlorine sensor (CLO 1-mA-2 ppm, ProMinent, Inc.) was 0.02–2.00 ppm with an uncertainty of ±0.02 ppm. The chlorine sensor was installed in a bypass loop equipped with a flow control valve and a flowrate measurement device (DGMa310T000, ProMinent, Inc.). The flowrate for the chlorine sensor was maintained at 60 L/hr regardless of flow conditions in the main pipeline system. The system measured chlorine concentration at a sampling rate of 1 Hz. The current signal from the residual chlorine sensor (4–20 mA) was sent to a data acquisition system and converted to a corresponding chlorine concentration (ppm). The potential effects of biofilm generation and other residuals were minimized by cleaning the pipeline system with detergent prior to each experiment. Tap water was also circulated through the pipeline system for 30 min, and the absence of residuals was confirmed before each experiment.

Transient flow events caused by closing the ball valve manually are difficult to regulate. To ensure uniform transient intensity for experimental purposes, a transient generator that can repeatedly generate identical events of various frequencies was designed, constructed and installed on the valve at the downstream end. The transient generator consists of a connection rod, a pneumatic cylinder, and a solenoid valve. One end of the connection rod was attached to the pneumatic cylinder, and the other was connected to the lever of the ball valve, which converted the linear motion of the cylinder into rotational motion of the ball valve (see Figure 1). The closing time of a transient generator can be set to 0.05–5.00 s. Pressure was measured at the adjacent upstream point of the control valve using the TP-1 monitoring system (Pipetech Int.). Sampling rates for the pressure were 10 Hz under steady state conditions and 100 Hz under transient conditions. Figure 1 shows a schematic and photographs of the pilot-scale water distribution system for the experiment.

Chlorine decay models

Table 1 presents existing models and their corresponding parameters for predicting chlorine decay in water distribution systems (Haas & Karra 1984). The first-order model is based on the assumption that the reaction rate is proportional to the residual chlorine concentration. The nth-order model is similar, but the decay rate in this model is proportional to the nth power of chlorine concentration. Limited models assume that some chlorine remains in the water unreacted. The parallel first-order model assumes that the overall rate of chlorine decay can be derived from the fast and slow components of the decay processes; therefore, the parallel first-order model consists of the weighted sum of two different first-order models.

To compile the approaches of these existing models into a generic model structure, this study introduces a comprehensive modeling framework based on the assumption that chlorine decay is controlled by one or more independent mechanism(s) that initiate simultaneously (Kim *et al.* 2015a). If m is the number of components in the decay of chlorine, then the rate of decrease of chlorine

Table 1 | Existing models for chlorine decay in water distribution systems

Title	Governing equation	Parameters
1st order	$C = C_0 \exp(-kt)$	k
2nd order	$C = \left(kt + \left(\frac{1}{C_0}\right)^{(1)}\right)^{-1}$	k
3rd order	$C = \left(2kt + \left(\frac{1}{C_0}\right)^{2}\right)^{-\frac{1}{2}}$	k
4th order	$C = \left(3kt + \left(\frac{1}{C_0}\right)^{3}\right)^{-\frac{1}{3}}$	k
Limited 1st order	$C = C_* + (C_0 - C_*) \exp(-kt)$	k
Limited 2nd order	$C = C_* + \left(kt + \left(\frac{1}{C_0 - C_*}\right)\right)^{-1}$	k, C_*
Limited 3rd order	$C = C_* + \left(2kt + \left(\frac{1}{C_0 - C_*}\right)^{2}\right)^{-\frac{1}{2}}$	k, C_*
Limited 4th order	$C = C_* + \left(3kt + \left(\frac{1}{C_0 - C_*}\right)^{3}\right)^{-\frac{1}{3}}$	k, C_*
Parallel 1st order	$C = w_1 C_0 \exp(-k_1 t) + (1 - w_1) C_0 \exp(-k_2 t)$	k_1, k_2, w_1

concentration over time can be determined by the summation of all reactants as

$$\frac{dC}{dt} = \frac{d}{dt}\left(\sum_{i=1}^{m} C_i\right) \quad (1)$$

where C_i is the concentration of the corresponding reactant i.

The reaction rate for each individual component can be generalized as

$$\frac{dC_i}{dt} = -k_i\left(C_i - C_i^*\right)^{n_i} \quad (2)$$

where k_i is the decay coefficient for ith reaction and n_i is the order of the corresponding reaction. The initial concentration of the corresponding partial concentration can be defined as

$$C_{i,0} = w_i C_0 \quad (3)$$

where w_i is the weighting of the ith reaction, and $\sum_{i=1}^{m} w_i = 1$, and C_o is the initial concentration of total chlorine. Equation (3) is the general formulation of the parallel first-order model.

Table 2 presents comprehensive models for five distinct formulations that incorporate existing model structures as well as their extensions. The nth- and limited nth-order models can be further generalized with an assumption that the parameters n and k are adjustable. The restriction of existing approaches of n as an integer is largely relaxed by defining n instead as a real number in the generic formulations. Further generalization of the nth and limited nth models can be made as the condition of two reactants is introduced; depending upon the scope of implementation of n as a real number into different decay processes, structures of a combined '$1+1$' model, a combined '$1+n$' model, and a combined '$n+n$' model can be developed (see Table 2).

Calibration of model parameters

In this study, the parameters of the chlorine decay models were calibrated using a GA (Goldberg 1989). The population and generation numbers were 100 and 100, respectively, and other GA parameters were determined based on the

Table 2 | Generic models for chlorine decay in water distribution systems

Title	Governing equation	Parameters
nth	$\mathrm{C} = \left((n-1)kt + \left(\frac{1}{C_0}\right)^{(n-1)}\right)^{-\frac{1}{n-1}}$	k, n
Limited nth	$\mathrm{C} = C_* + \left((n-1)kt + \left(\frac{1}{C_0 - C_*}\right)^{(n-1)}\right)^{-\frac{1}{n-1}}$	k, n
Combined '$1+1$'	$\mathrm{C} = C_* + w_1(C_0 - C_*)\exp(-k_1 t) + (1-w_1)(C_0 - C_*)\exp(-k_2 \mathrm{t})$	$k_1,\ k_2, C^*, w_1$
Combined '$1+n$'	$\mathrm{C} = C_* + w_1(C_0 - C_*)\exp(-k_1 t) + \left(k_2 t(n_2-1) + \left(\frac{1}{(1-w_1)(C_0 - C_*)}\right)^{(n_2-1)}\right)^{-\frac{1}{n_2-1}}$	$k_1,\ k_2, n_2, C^*, w_1$
Combined '$n+n$'	$\mathrm{C} = C_* + \left(k_1 t(n_1-1) + \left(\frac{1}{w_1(C_0 - C_*)}\right)^{(n_1-1)}\right)^{-\frac{1}{n_1-1}} + \left(k_2 t(n_2-1) + \left(\frac{1}{(1-w_1)(C_0 - C_*)}\right)^{(n_2-1)}\right)^{-\frac{1}{n_2-1}}$	$k_1, k_2, n_1, n_2, C^*, w_1$

recommendations of Goldberg (1989). The objective function of this study was to minimize the RMSE between the chlorine concentrations predicted with the selected model and the observed values. The following equation represents this objective function:

$$RMSE = \sqrt{\sum_{i=1}^{n} (C_{obs}(i) - C_{\mathrm{model}}(i,\ p_1,\ p_2, \ldots, p_k))} \quad (4)$$

where i is the time step, $C_{obs}(i)$ is the observed chlorine concentration, $C_{Model}(i, p_1, p_2 \ldots p_k)$ is the predicted chlorine concentration from a selected model, and p_k represents parameters for a generic model.

Transient analysis in the pipeline

Two-dimensional analysis was conducted to determine the radial variations in hydraulic conditions during transient events. Figure 2 illustrates a cylindrical grid element of the pipe that was used for modeling. Because the water pressure of the system drops below the vapor pressure of the water during transient events, a transient vaporous cavitation model was adopted for this study.

The governing equation of the mathematical model for these transient events proposed by Pezzinga & Cannizzaro (2014) is shown in Equations (5) and (6):

$$\frac{\partial \varphi}{\partial t} + \frac{a^2}{g}\frac{\partial V}{\partial x} = 0 \quad (5)$$

$$\frac{\partial u}{\partial t} + g\frac{\partial H}{\partial x} + \frac{1}{\rho r}\frac{\partial (r\tau)}{\partial r} = 0 \quad (6)$$

where $t =$ time, $a =$ wave speed (1,395 m/s), g = gravitational acceleration, V is the mean flow velocity calculated as $V = \int_0^{r_0} 2\pi rudr/A$, r_0 is the radius of the pipe, $H = z + p/\rho_i g$ is the piezometric head, $\tau =$ wall shear stress which can be determined as in Zhao & Ghidaoui (2003), and ρ represents the density of the liquid–vapor mixture, which can be calculated as $\rho = \rho_l(1 - \alpha_v)\rho_v\alpha_v$. An auxiliary variable φ, which represents the piezometric head adjusted for vaporous cavitation, can be defined as

$$\varphi = \frac{p}{\rho_l g} + \frac{a^2}{g}\ln(1 - \alpha_v) \quad (7)$$

where $\rho_l =$ liquid density, and $\alpha_v =$ volume of vapor/total volume. Pressure (p) and vapor fraction (α_v) can be calculated using Equation (8):

$$p = \max(\rho_l g\varphi, p_v) \quad (8)$$

To solve Equations (5) and (6), a numerical algorithm based on a predictor–corrector method was used (MacCormack 2003). Equations (9) and (10) are the differentiated forms of predictor–corrector schemes:

$$\begin{aligned} &\frac{\varphi_i^p - \varphi_i^{n-1}}{\Delta t} + \frac{a^2}{g}\frac{V_{i+1}^{n-1} - V_i^{n-1}}{\Delta x} = 0 \\ &\frac{u_{i,j}^p - u_{i,j}^{n-1}}{\Delta t} + g\frac{H_{i+1}^{n-1} - H_i^{n-1}}{\Delta x} + \frac{2\pi}{\rho}\frac{(r_{j+1}\tau_{i,j+1}^* - r_j\tau_{i,j}^*)}{\Delta A} = 0 \end{aligned} \quad (9)$$

$$\begin{aligned} &\frac{\varphi_i^c - \varphi_i^{n-1}}{\Delta t} + \frac{a^2}{g}\frac{V_i^p - V_{i-1}^p}{\Delta x} = 0 \\ &\frac{u_{i,j}^c - u_{i,j}^{n-1}}{\Delta t} + g\frac{H_i^p - H_{i-1}^p}{\Delta x} + \frac{2\pi}{\rho}\frac{(r_{j+1}\tau_{i,j+1}^* - r_j\tau_{i,j}^*)}{\Delta A} = 0 \end{aligned} \quad (10)$$

and i, j, and n are the indices of longitudinal, radial, and time, respectively, at p and c which represent the predictor–corrector step and τ^* is the average of shear stress between the predictor and corrector step.

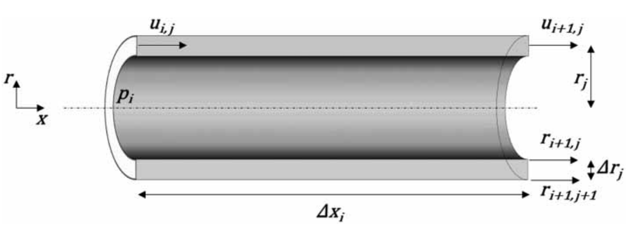

Figure 2 | A schematic for two-dimensional modeling of a cylindrical grid element of the pipe.

Turbulence intensity

Turbulent flow in a real-life system is based on the unpredictable variation of flow velocity and pressure. It is impossible to calculate the intensity of the turbulence at a certain time and location with either a 1D or 2D simulation model. In this regard, turbulence simulations should be performed statistically, where the statistical mechanics of ensemble average technique are integrated. Possible fluctuations of velocity are produced intentionally by minor modifications of initial velocity. In this study, N_{en} sets of numerical simulations were conducted with minor differences in initial flow velocity. The ensemble average of velocity ($\bar{u}$) can be expressed as follows:

$$\bar{u} = \frac{1}{N_{en}} \sum_{i=1}^{N_{en}} u_i \tag{11}$$

where $\bar{u}$ is the ensemble average of velocity, N_{en} is the number of ensemble sets with different initial flow velocities and u_i is the velocity dependent on time and location. The ensemble average of velocity is a representative value that is independent from system uncertainty. The difference between an ensemble average of velocity ($\bar{u}$) and a velocity of the ith component of an ensemble set (u_i) is the velocity fluctuation (u'_i) of the ith component and can be expressed as follows:

$$u'_i = u_i - \bar{u} \tag{12}$$

The strength of turbulence can be expressed as the root mean square quantity of the velocity fluctuation and can be written as follows:

$$T_{strength} = u_{rms} = \sqrt{\frac{1}{N_{en}} \sum_{i=1}^{N_{en}} (u'_i)^2} \tag{13}$$

where $T_{strength}$ is the strength of turbulence, u_{rms} represents the standard deviation of the velocity fluctuation and u'_i is the velocity fluctuation at the ith component of the ensemble set.

Turbulence intensity (I) is the relative quantity of the standard deviation of the velocity fluctuation to the mean flow velocity, which can be expressed as follows:

$$I = \frac{u_{rms}}{\bar{u}} \tag{14}$$

where $\bar{u}$ is the mean velocity $\bar{u} = 1/N_{en} \sum_{i=1}^{N_{en}} u_i$.

The integrated turbulence intensity accumulated over time t ($\bar{I}_t$) and the difference in accumulated turbulence intensity between the steady state and a transient event ($\Delta\bar{I}_t$) are expressed by Equations (15) and (16), respectively:

$$\bar{I}_t = \int_0^t I dt \tag{15}$$

$$\Delta\bar{I}_t = \bar{I}_{t,steady} - \bar{I}_{t,transient} \tag{16}$$

where I is the turbulence intensity at time t, and $\bar{I}_{t,steady}$ and $\bar{I}_{t,transient}$ are $\bar{I}_t$ under steady and transient conditions, respectively, for time step t.

The total amount of the reduction of turbulence intensity caused by transient events at time t (I_T) can be calculated using Equation (17):

$$I_T = \sum_{l=1}^{N} \Delta\bar{I}^{l}_{t(l)} \tag{17}$$

where l and $t(l)$ represent a particular transient event and its duration for the lth event, respectively, and N is the number of transient events.

RESULTS

Transient event introduction and chlorine concentrations

A transient event can be introduced into the experimental pipeline system by closing the valve over 0.2 seconds. The transient generator can regulate sequential transients for various frequencies (once every 40, 20, 10, 5, and 2.5 min) from a 1.6 m/s steady flow state. The steady pressure head was maintained at 4.1 m, and the maximum pressure head during transient events was 183.5 m. Chlorine concentration data in a range of 2.0–0.2 ppm were collected at a frequency of 1 Hz. Figure 3 presents a time series for the transient pressure head introduced by instantaneous valve closure.

Figure 4 shows variations in chlorine concentrations under steady conditions and several different transient conditions. Chlorine concentration tends to decreased more rapidly under steady conditions than under unsteady

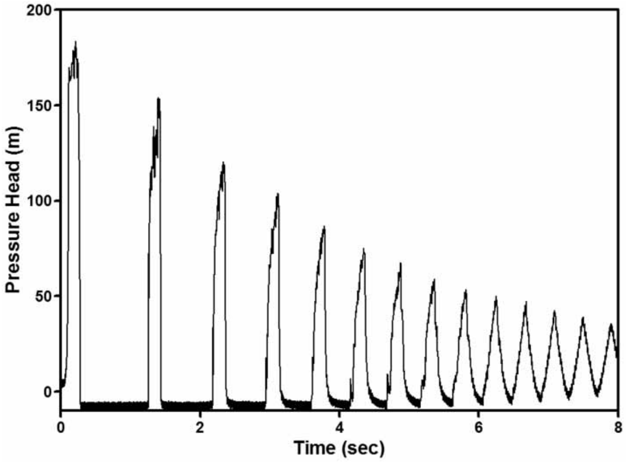

Figure 3 | Time series of pressure head values during a single transient event.

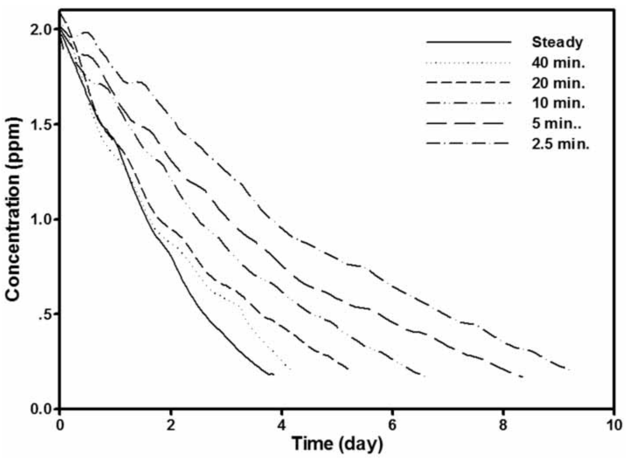

Figure 4 | Chlorine concentrations under steady and unsteady conditions with transient events every 40, 20, 10, 5, and 2.5 min.

conditions. The periods required for 90% reduction in chlorine concentration (from 2.0 to 0.2 mg/L) were 3.86 days under steady conditions, and 4.19, 5.20, 6.58, 8.35 and 9.25 days for unsteady conditions with transients produced at intervals of 40, 20, 10, 5, and 2.5 min, respectively.

Calibration of chlorine decay model parameters

Parameter calibration results for models in Tables 1 and 2 are presented in Table 3. Calibrations were performed through three distinct model structures: the designation of the reaction order (n) as an integer for Equation (2) (e.g., models 1–9 in Table 3), calibration incorporating parameter n as a real number (e.g., models 10 and 11 in Table 3), and the most comprehensive calibration involving a flexible concentration of the stable component (c^*) instead of a designated c^* for a lower detection limit of the sensor (e.g., models 12–14 in Table 3).

Parameter k tended to decrease with increasing transient generation frequency for models 1–8 in Table 3. These results reflect the temporal variation of chlorine concentration under different hydraulic conditions as shown in Figure 4. The weighting factor of model 9 also decreased with increasing transient frequency. However, because the parameters k_1 and k_2 of model 9 were almost identical to parameter k of model 1, the overall structure of model 9 is very similar to that of model 1. This similarity suggests that regardless of hydraulic conditions, assuming a first-order reaction for both the rapid initial decay and the slower and prolonged decay for the parallel first-order model is not appropriate.

Regarding models 10 and 11, the optimal n values for the nth-order and the limited nth-order models under steady flow conditions were 0.407 and 0.390, respectively. These values indicate that the chlorine decay rate was less sensitive to residual chlorine in this system than in other existing models. Optimal n and k under transient conditions both decreased as the water-hammer frequency is increased, which represents overall decline in the chlorine decay rate. This trend suggests that this transient-induced phenomenon may mitigate the consumption of chlorine.

Model 12 combines two limited first-order decay models with different rate constants. Because the model is flexible for the parameter c^*, it can be simplified into model 1, 5 or 9 depending on the values of the parameters. The calibrated value of c^* for all hydraulic conditions was determined to be zero, and the values of the corresponding rate coefficients k_1 and k_2 were almost the same. The structure of model 12 in this study was ultimately similar to the structure of model 1. This similarity indicates that model 1 performed best among models 1, 5, 9, and 12, considering that it is desirable to minimize differences between observational and modeling results with the minimum number of parameters for calibration with an evolutionary algorithm.

The weighting parameters of model 13 for all hydraulic conditions in this study were small ($w < 0.5$). This finding

Table 3 | Calibrated parameters for candidate chlorine models with different hydraulic conditions

Model	Title	Parameter	Steady	40 min	20 min	10 min	5 min	2.5 min
1	1st order	k (day^{-1})	0.479	0.440	0.397	0.286	0.240	0.185
2	2nd order	k (day^{-1})	0.392	0.357	0.330	0.238	0.201	0.141
3	3rd order	k (day^{-1})	0.318	0.285	0.270	0.195	0.166	0.105
4	4th order	k (day^{-1})	0.260	0.244	0.244	0.163	0.139	0.078
5	Limited 1st order	k (day^{-1})	0.488	0.458	0.397	0.292	0.244	0.188
6	Limited 2nd order	k (day^{-1})	0.406	0.366	0.336	0.246	0.208	0.145
7	Limited 3rd order	k (day^{-1})	0.334	0.305	0.275	0.206	0.175	0.110
8	Limited 4th order	k (day^{-1})	0.278	0.250	0.250	0.175	0.156	0.084
9	Parallel 1st order	w	0.995	1.000	0.851	0.753	0.711	0.652
		k_1 (day^{-1})	0.468	0.440	0.400	0.288	0.240	0.184
		k_2 (day^{-1})	0.480	0.439	0.390	0.283	0.240	0.185
10	nth order	n	0.407	0.997	0.967	0.563	0.701	0.507
		k (day^{-1})	0.527	0.437	0.401	0.305	0.250	0.213
11	Limited nth order	n	0.390	0.980	0.945	0.547	0.683	0.478
		k (day^{-1})	0.531	0.437	0.409	0.309	0.254	0.214
12	Combined '1 + 1'	w	0.942	0.992	0.959	0.903	0.859	0.792
		k_1 (day^{-1})	0.479	0.440	0.399	0.287	0.240	0.185
		k_2 (day^{-1})	0.478	0.440	0.390	0.276	0.238	0.185
		c^* (mg/L)	0.000	0.000	0.000	0.000	0.000	0.000
13	Combined '1 + n'	w	0.125	0.332	0.314	0.259	0.083	0.015
		k_1 (day^{-1})	0.407	0.995	0.974	0.248	0.082	0.057
		n	0.348	0.131	0.348	0.423	0.571	0.573
		k_2 (day^{-1})	0.500	0.291	0.279	0.279	0.277	0.211
		c^* (mg/L)	0.020	0.029	0.040	0.040	0.072	0.072
14	Combined '$n + n$'	w	0.424	0.304	0.261	0.204	0.192	0.191
		n_1	0.375	0.878	0.804	0.604	0.582	0.165
		k_1 (day^{-1})	0.255	0.998	0.856	0.211	0.190	0.060
		n_2	0.364	0.069	0.433	0.501	0.628	0.651
		k_2 (day^{-1})	0.438	0.295	0.295	0.263	0.219	0.187
		c^* (mg/L)	0.034	0.003	0.011	0.032	0.037	0.045

reflects that the nth (<1) order is the dominant form of modeling, and this trend intensified as the frequency of transient events was increased. Positive correlation was also found between the c^* values of model 13 and the frequency of transient events, which means that the reactivity of chlorine compounds decreased with the occurrence of transient events. The generation of transient events, therefore, is found to inhibit the consumption of chlorine.

A positive effect of transient events on the concentration of stable component c^* was shown in model 14 as well. This model combines an n_1th-order model with the decay coefficient k_1 with an n_2th-order model with the decay coefficient k_2. The optimal balance between the n_1th-order model and n_2th-order model was determined through the modeling results. The weighting parameter w and the n_1th-order parameters n_1 and k_1 decreased with increased transient event frequency, but the converse was observed for the order n_2.

Table 4 shows that for all models used for calibration, the degrees of fitness in terms of RMSEs and coefficients of determination (R^2) were similar under both steady and unsteady conditions for each model. Figure 5 shows the means and standard errors of RMSE for all candidate chlorine decays models.

As shown in Table 4, the low-order existing models (i.e., first-, limited first-, and parallel first-order) show relatively

Table 4 | Determination coefficients (R^2) and RMSEs of the models

Frequency of transient event		Steady		40 min		20 min		10 min		5 min		2.5 min	
Model	**Title**	R^2	RMSE	R^2	RMSE	R^2	RMSE	R^2	RMSE	R^2	RMSE	R^2	RMSE
1	1st order	0.97	0.099	0.99	0.044	1.00	0.026	0.98	0.074	0.99	0.055	0.97	0.099
2	2nd order	0.87	0.203	0.93	0.137	0.94	0.131	0.89	0.181	0.90	0.168	0.88	0.201
3	3rd order	0.76	0.273	0.83	0.209	0.84	0.212	0.78	0.253	0.79	0.245	0.78	0.270
4	4th order	0.66	0.323	0.74	0.263	0.73	0.272	0.68	0.304	0.69	0.300	0.68	0.320
5	Limited 1st order	0.97	0.102	0.99	0.048	1.00	0.031	0.98	0.077	0.99	0.058	0.97	0.102
6	Limited 2nd order	0.86	0.206	0.93	0.140	0.93	0.135	0.88	0.184	0.90	0.172	0.87	0.204
7	Limited 3rd order	0.84	0.225	0.90	0.165	0.90	0.168	0.86	0.201	0.88	0.189	0.82	0.241
8	Limited 4th order	0.65	0.326	0.73	0.265	0.73	0.275	0.67	0.307	0.68	0.304	0.68	0.323
9	Parallel 1st order	0.97	0.099	0.99	0.044	1.00	0.025	0.98	0.074	0.99	0.055	0.97	0.099
10	*n*th order	1.00	0.026	0.99	0.044	1.00	0.025	1.00	0.027	1.00	0.026	0.99	0.054
11	Limited *n*th order	1.00	0.026	0.99	0.048	1.00	0.025	1.00	0.027	1.00	0.026	0.99	0.049
12	Combined '1 + 1'	0.97	0.099	0.99	0.044	1.00	0.025	0.98	0.074	0.99	0.055	0.97	0.099
13	Combined '1 + n'	1.00	0.026	1.00	0.026	1.00	0.023	1.00	0.028	1.00	0.025	0.99	0.056
14	Combined 'n + n'	1.00	0.023	1.00	0.025	1.00	0.021	1.00	0.027	1.00	0.025	0.99	0.051

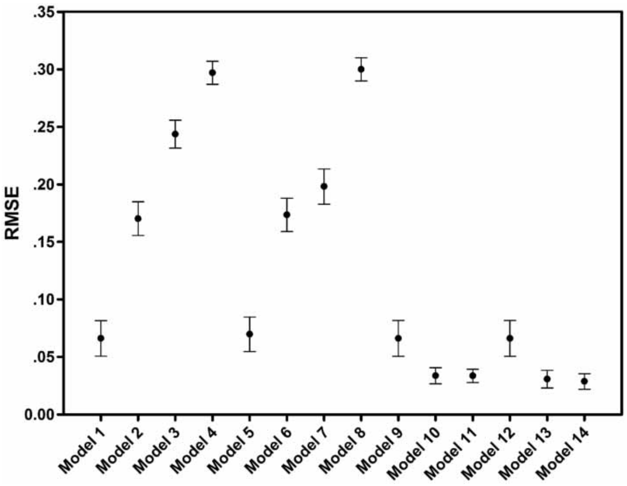

Figure 5 | Means and standard deviations of RMSE for all candidate chlorine decay models.

high fitness compared to the high-order existing models (i.e., second-, third-, fourth-, limited second-, limited third-, and limited fourth-order). This finding can be explained by the characteristics of the experimental data and the structures of the models. High-order models have advantages for prediction of steep declines from the initial chlorine concentration, which is suitable for representing rapid chlorine decay. However, because organic compounds were not added for this experiment, chlorine was consumed more gradually by the low levels of organics typical for drinking water.

R^2 values for the generic models were higher, the corresponding RMSEs were lower, and corresponding standard errors were narrower than those for other models (see Table 4). This means that an additional degree of freedom in the reaction order (n_i) has great potential to enable better estimates of chlorine decay behavior under both steady and unsteady conditions. Chlorine decay behavior conditions can therefore be successfully modeled using the structures of Equations (1), (2), and (3) for either steady or unsteady flow conditions, provided that the variability of other factors (e.g., temperature, service age, and concentration of organics) can be controlled. These findings suggest that there is no universal chlorine decay model that is suitable for all system conditions. As the number of adjustable parameters increases, models have more flexibility to fit chlorine decay under a variety of conditions.

DISCUSSION

Transient event impact on the chlorine decay process

In order to evaluate the underlying processes of chlorine decay in conjunction with varying flow regimes, Equations (5)–(10) were employed to model temporal and spatial flow variations in two-dimensional space (see Figure 2). Numerical results obtained with Equations (9) and (10) are displayed in Figure 6; these results show strong agreement with the experimental data. Figure 7(a) and 7(b) illustrate the velocity profiles obtained with the numerical model under steady state and transient conditions, respectively. The velocity profiles for 10, 20, 30, 40, and 50 m from the water tank under steady state conditions (see Figure 7(a)) indicate that radial velocity profiles were developed from the water tank, and that almost fully developed velocity distribution was reached by the 50 m point.

Figure 7(b) presents radial velocity profiles with different times (in terms of $2L/a$ where L is the length of the pipeline and a is the wave speed) for a point 50 m from the water tank. As shown in the velocity profile for $8.25{\cdot}2L/a$, flow separation can be generated. Flow reversal was observed in the velocity profile for $8.25{\cdot}2L/a$ after a transient event, which implies the occurrence of an adverse pressure gradient near the wall region.

In order to calculate turbulence intensity, the model has been repeated 200 times to generate white noise through variation in the initial velocity (Shamloo & Mousavifard

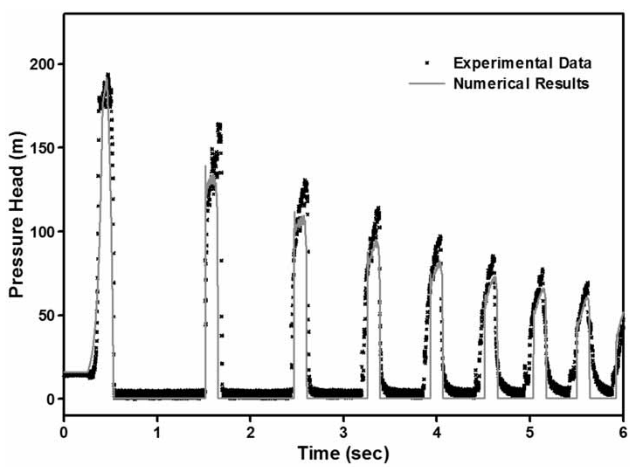

Figure 6 | Observed and simulated pressures using a two-dimensional flow model.

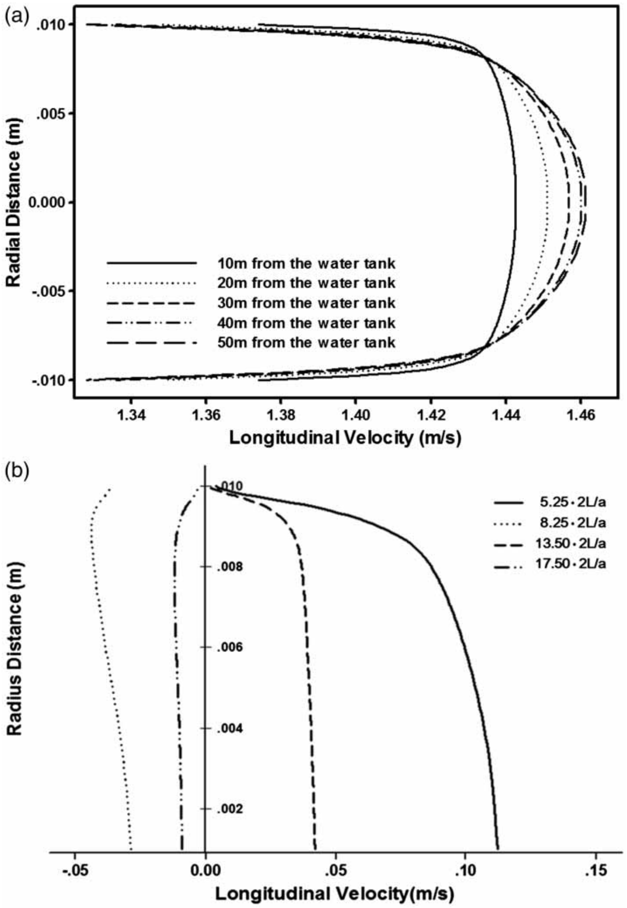

Figure 7 | Velocity profiles under steady state conditions for (a) different points and (b) with a transient event at a point 50 m from the water tank.

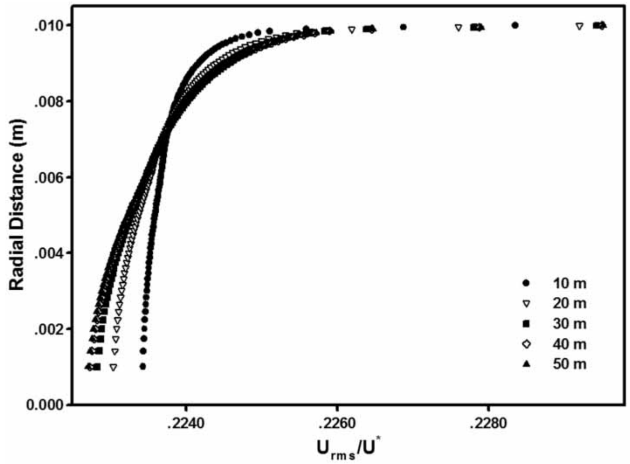

Figure 8 | Distributions of turbulence intensity under steady state conditions at different points.

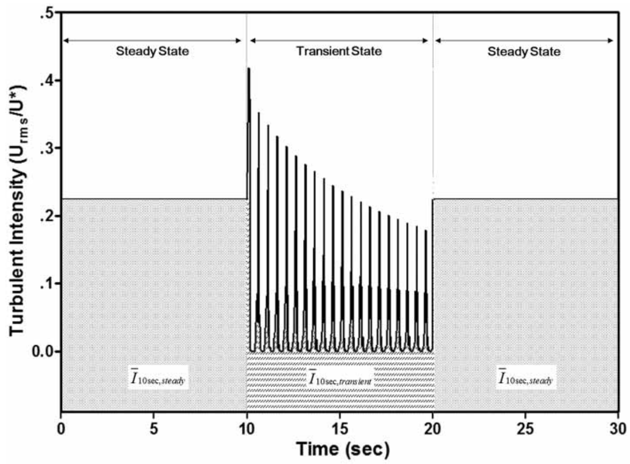

Figure 9 | Temporal variation of turbulence intensity over 10 seconds of a transient event at a point 5 m from the end valve.

2015). Figure 8 shows the radial variation of turbulence intensity in the steady state and after a transient event. Turbulence intensity at or near the pipe wall is generally higher than that at the centerline because of high shear stress near the wall (Kita *et al.* 1980). The turbulence intensity gradient tends to become pronounced as the velocity profile develops (see Figure 8); however, the standard deviation and mean of radial turbulence intensity distribution, respectively, were 0.00067 and 0.22379, which means that there is no significant difference in the intensity of turbulence between the wall and the centerline area in this system because of the pipe's small diameter. Figure 9 shows the temporal variation of averaged radial turbulence intensity during a single transient event at a point 5 m from the end valve. During the transient event, the averaged radial turbulence intensity of the system fluctuated from zero to about two times the steady state value. As the closed valve is opened at the end of the transient event, the negligible turbulent intensity is increased to that of steady state flow. The highest value of turbulence intensity was observed after valve closure, when the average standard deviation and the mean of the radial distribution of turbulence intensity during a transient event were 0.0000524 and 0.041939, respectively.

With the structure of the experimental pipeline system, the amount of turbulence intensity reduction by a single transient event ($\Delta\overline{I_{10\,sec}}$) was about 1.822. Data for chlorine concentration under different hydraulic conditions over 4 days were used to compare the rate of chlorine decay. In this study, each transient event has an identical total turbulent intensity that is repeated every 10 seconds. Therefore, Equation (17) can be simplified as follows:

$$I_T = N \times \Delta \bar{I}_{10\,\mathrm{sec}} \tag{18}$$

Table 5 summarizes the total number of transient events over 4 days and the corresponding total amount of turbulence intensity reduction. The total reduction of turbulence intensity, I_T, increased as the interval between transient events interval was decreased.

Power regressions of I_T versus the parameters of chlorine decay models are presented in Table 6. The parameters of existing models are affected negatively by I_T and show strong correlations ($R^2 > 0.86$). The parameter a (the proportional coefficient of regression equation) tends to decrease as the order n increases for the nth-order and limited nth-order models, and the converse tendency is apparent for the parameter b (the power coefficient of regression equation), except in the case of the fourth-order model, for which R^2 values are small relative to those of other models (see Table 6).

In addition, we report that regression equations provide adequate estimations of chlorine decay through the total reduction of turbulence intensity. Regression equations and validation results of the parameters for the parallel first-order model and combined '1 + 1' model were similar to those for the first-order model. Although the nth- and limited nth-order models show weak correlations with I_T, the fitness of these models, using parameters obtained from the regression equations is generally favorable. As I_T is increased, the parameter w of the combined '$1 + n$' model tends to decrease; i.e., the combined '$1 + n$' model tends to be governed by the nth-order model as transient events are introduced into system. The parameter c^* of the combined '$1 + n$' and combined '$n + n$' models tends to decrease as the value for I_T is increased, which means that the amount of unreactive chlorine is increased with decreasing turbulence intensity.

Degrees of fitness (in terms of R^2 and RMSE) of modeling calculated using the parameters obtained from the regression equations in Table 6 are presented in Table 7. R^2s and RMSEs for the nth-order and limited nth-order models tend to decrease and increase, respectively, as the order n of the models is increased. Both R^2 and RMSE for the five generic models (from the nth-order model to the combined '$n + n$' model) are generally superior to the nine existing models. These findings indicate that the introduction of additional calibration parameters and relaxation limitations to chlorine decay order in model structure improve the predictability of chlorine decay behavior substantially even in modeling considering turbulence intensity for parameter evaluation. Chlorine decay models with low order ($n \leq 1$) showed good performance in terms of predictability and parsimony of model parameter than those for high order models.

Table 5 | Total turbulence intensity reduction ($\Delta \bar{I}_{10\,\mathrm{sec}} = 1.822$)

Transient event interval	Number of transient event during 4 days (N)	Total amount of turbulence intensity reduction ($I_{10\,\mathrm{sec}} = N \times \Delta \bar{I}_{10\,\mathrm{sec}}$)
Steady state (No transient event)	0	0
40 min	151	274.8997
20 min	375	682.717
10 min	948	1,727.655
5 min	2,404	4,379.447
2.5 min	5,330	9,712.182

Chlorine decay under transient conditions

In this study, time series of residual chlorine concentrations under steady and transient conditions were obtained from a pilot-scale water distribution system. Although different pipeline materials were used, the evaluated chlorine decay rates showed similar trends to those reported by Ramos *et al.* (2010), i.e., that the chlorine decay rates under unsteady flow conditions are lower than those under steady flow conditions. However, this study further investigated the effects of transient events on the decay rates of chlorine compounds through the application of diverse event frequencies and through two-dimensional flow analyses with respect to the relationships between turbulence intensity and chlorine decay processes.

Generic models for chlorine decay that were previously proposed by Kim *et al.* (2015a) for steady flow conditions were used in this study. Based on the proposed models, a calibration range for the parameter n was extended to real numbers, instead of limited to integers, and the concentration of the stable component (c^*) was evaluated as an

Table 6 | Regression equations between I_T and model parameters (y) using $y = ax^b$ and the corresponding determination coefficients (R^2) for all models

Model	y	X	a	b	R^2
1st order	k	I_T	1.869	-2.487×10^{-1}	0.980
2nd order	k	I_T	1.670	-2.611×10^{-1}	0.958
3rd order	k	I_T	1.474	-2.741×10^{-1}	0.928
4th order	k	I_T	1.657	-3.143×10^{-1}	0.892
Limited 1st order	k	I_T	1.951	-2.519×10^{-1}	0.988
Limited 2nd order	k	I_T	1.677	-2.578×10^{-1}	0.959
Limited 3rd order	k	I_T	1.557	-2.750×10^{-1}	0.936
Limited 4th order	k	I_T	1.498	-2.925×10^{-1}	0.861
Parallel 1st order	w	I_T	1.845	-1.151×10^{-1}	0.968
	k_1	I_T	1.892	-2.500×10^{-1}	0.978
	k_2	I_T	1.827	-2.463×10^{-1}	0.983
nth	n	I_T	2.868	-1.861×10^{-1}	0.740
	k	I_T	1.494	-2.118×10^{-1}	0.983
Limited nth	n	I_T	2.978	-1.952×10^{-1}	0.751
	k	I_T	1.513	-2.120×10^{-1}	0.977
Combined '1 + 1'	w	I_T	1.426	-6.217×10^{-1}	0.975
	k_1	I_T	1.878	-2.491×10^{-1}	0.978
	k_2	I_T	1.834	-2.477×10^{-1}	0.980
	w	I_T	61.96	-8.330×10^{-1}	0.790
Combined '1 + n'	k_1	I_T	230.3	-9.147×10^{-1}	0.941
	n	I_T	0.02066	3.857×10^{-1}	0.816
	k_2	I_T	0.4503	-7.087×10^{-1}	0.596
	c*	I_T	0.0066	2.653×10^{-1}	0.901
	w	I_T	0.6310	-1.379×10^{-1}	0.892
Combined 'n + n'	n_1	I_T	10.39	-4.009×10^{-1}	0.717
	k_1	I_T	104.2	-7.918×10^{-1}	0.925
	n_2	I_T	0.006321	5.443×10^{-1}	0.680
	k_1	I_T	0.6737	-1.344×10^{-1}	0.915
	c^*	I_T	6×10^{-5}	7.537×10^{-1}	0.855

adjustable parameter instead of a fixed value to compensate for various hydraulic conditions. Among the 14 candidate models, the combined '$n + n$' model yielded the best performance for fitting chlorine concentration data. The concentration of c^* decreased as the transient event frequency increased for combined '$n + n$' model (Table 3), which indicates that the reactivity of chlorine compounds tends to decrease with the introduction of transient events into the system.

This phenomenon can be explained based on the influence of turbulence intensity on the interaction of chlorine in bulk water with biofilm along the pipe wall (Percival *et al.* 2000). Turbulence intensity in the early period of the water hammer, at 2.5 L/a where L is pipeline length and a is wave speed, is greater than that under steady flow conditions, but it decreases over time (Shamloo & Mousavifard 2015). We used a closed valve for about 10 sec, which is approximately equal to the period of 100 L/a. Therefore, overall turbulence intensity was substantially lower than the intensity under steady flow conditions. As shown in Figure 9, the total turbulence intensity under transient events was less than that under steady flow conditions. From the perspective of collision theory, the chlorine compounds in a system with lower turbulence have fewer chances to react with reactants compared to those in systems with higher turbulence (Hahn 1994). Therefore, the regulation of transients can be considered as an alternative control to reduce chlorine decay of treated water in water distribution systems.

Table 7 | Validation of power regression equations

I_t	274.90		682.72		1,727.66		4,379.45		9,712.18	
Title	R^2	RMSE	R^2	RMSE	R^2	RMSE	R^2	RMSE	R^2	RMSE
1st order	0.99	0.055	0.99	0.056	0.98	0.076	0.99	0.059	0.97	0.101
2nd order	0.92	0.141	0.93	0.136	0.89	0.181	0.90	0.171	0.87	0.204
3rd order	0.83	0.212	0.83	0.215	0.78	0.253	0.79	0.249	0.77	0.274
4th order	0.72	0.269	0.73	0.271	0.68	0.304	0.69	0.303	0.68	0.324
Limited 1st order	0.99	0.059	0.99	0.055	0.98	0.079	0.99	0.062	0.97	0.103
Limited 2nd order	0.92	0.143	0.93	0.141	0.88	0.184	0.90	0.175	0.87	0.207
Limited 3rd order	0.92	0.148	0.87	0.186	0.85	0.206	0.84	0.218	0.86	0.216
Limited 4th order	0.72	0.269	0.73	0.275	0.67	0.307	0.68	0.306	0.67	0.328
Parallel 1st order	0.99	0.056	0.99	0.055	0.98	0.076	0.99	0.059	0.97	0.099
*n*th order	0.99	0.050	0.98	0.066	0.99	0.044	1.00	0.026	0.99	0.056
Limited *n*th order	0.99	0.049	0.98	0.071	0.99	0.042	1.00	0.026	0.99	0.054
Combined '$1+1$'	0.99	0.051	0.98	0.067	0.98	0.077	0.98	0.066	0.97	0.102
Combined '$1+n$'	0.99	0.051	0.95	0.117	0.97	0.090	0.99	0.062	0.97	0.102
Combined '$n+n$'	1.00	0.030	0.97	0.084	0.99	0.048	1.00	0.032	0.98	0.085

CONCLUSIONS

Hydraulic transients in a pipeline system introduce changes to the flow regime and affect residual chlorine concentrations. The impacts of transient events on the mechanisms of chlorine decay had not previously been systematically explored using a pilot-scale water distribution system. Therefore, to investigate chlorine concentration behavior comprehensively, general model frameworks were introduced and integrated into GAs for parameter calibration. The proposed model structure showed better fitness than existing models, which was achieved based on the relaxation of reaction order and concentration of the stable component in calibration. The first order model provided good performance both in predictability and model parsimony. Calibrated parameters yielded higher decay coefficients for steady flow than for unsteady flow conditions, and lower decay coefficients were calculated for hydraulic conditions with transient events at shorter intervals. Two-dimensional analysis of transient flow was conducted to evaluate the impact of turbulence intensity on the chlorine decay process. Decreased turbulence intensity with the introduction of transient events into the system is responsible for the observed reduction in chlorine decay, which can further be explained as the reduction of chlorine reaction with reactants. The strong relationships between the reduction of turbulence intensity and chlorine decay coefficients, as well as the high level of fitness of the simulations of chlorine concentrations using model parameters under transient conditions, highlight the impact of transient events on chlorine decay, and demonstrate that they can be successfully modeled in water distribution systems.

ACKNOWLEDGEMENTS

This research is supported by Korea Ministry of Environment as 'Global Top Project (RE201606133)'.

REFERENCES

Abokofa, A. A., Yang, Y. J., Lo, C. S. & Biswas, P. 2016 Water quality modeling in the dead end sections of drinking water distribution networks. *Water Research* **89**, 107–117.

Aisopou, A., Stoianov, I. & Karney, B. 2014 Analytical and experimental investigation of chlorine decay in water supply systems under unsteady hydraulic conditions. *Journal of Hydroinfomatics* **16**, 690–709.

Al-Jasser, A. O. 2007 Chlorine decay in drinking-water transmission and distribution systems: pipe service age effect. *Water Research* **41**, 387–396.

Al-Jasser, A. O. 2011 Pipe service age effect on chlorine decay in drinking-water transmission and distribution systems. *Clean Soil Air Water* **39**, 827–832.

Courtis, B. J., West, J. R. & Bridgeman, J. 2009 Temporal and spatial variations in bulk chlorine decay within a water supply system. *Journal of Environmental Engineering* **135**, 147–152.

Environmental Protection Agency (EPA) 2005 *Water Distribution System Analysis: Field Studies, Modeling and Management. EPA/600/R-06/028*, Cincinnati, OH, USA.

Fernandes, C. & Karney, B. 2004 Modelling the advection equation under water hammer conditions. *Urban Water Journal* **1**, 97–112.

Goldberg, D. E. 1989 *Genetic Algorithms in Search Optimization and Machine Learning*. Addison-Wesley, Boston, MA, USA.

Haas, C. N. & Karra, S. B. 1984 Kinetics of wastewater chlorine demand exertion. *Journal of Water Pollution Control Federation* **56**, 170–173.

Hahn, Y. B. 1994 A collision model for fine particles in a turbulent system. *Korean Journal of Chemical Engineering* **11**, 246–253.

Hallam, N. B., Hua, F., West, J. R., Forster, C. F. & Simms, J. 2003 Bulk decay of chlorine in water distribution systems. *Journal of Water Resources Planning and Management* **129**, 78–81.

Hoskins, A. & Stoianov, I. 2014 A distributed system for the continuous analysis of hydraulic transients. *Procedia of Engineering* **70**, 823–832.

Hua, F., West, J. R., Barker, R. A. & Forster, C. F. 1999 Modeling of chlorine decay in municipal water supplies. *Water Research* **33** (12), 2735–2746.

Hua, P., Vasyukoua, E. & Uhi, W. 2015 A variable reaction rate model for chlorine decay in drinking water due to the reaction with dissolved organic matter. *Water Research* **75**, 109–122.

Jadas-Hecart, A., El, M. A., Stitou, M., Bouillot, P. & Legube, B. 1992 The chlorine demand of a treated water. *Water Research* **26**, 1073–1084.

Kiene, L., Lu, W. & Levi, Y. 1998 Relative importance of the phenomena responsible for chlorine decay in drinking water distribution systems. *Water Science and Technology* **38** (6), 219–227.

Kim, H., Kim, S. & Koo, J. 2015a A general framework of chlorine decay modeling at a pilot scale water distribution system. *Journal of Water Supply: Research and Technology-AQUA* **64**, 543–557.

Kim, H., Kim, S. & Koo, J. 2015b Modelling chlorine decay in a pilot scale water distribution system subjected to transient. *Procedia of Engineering* **119**, 370–378.

Kita, Y., Adachi, Y. & Hirose, K. 1980 Periodically oscillating turbulent flow in a pipe. *Bulletin of the JSME* **23**, 656–664.

LeChevalier, M. W. 1990 Coliform regrowth in drinking water: a review. *Journal of American Water Works Association* **82**, 74–86.

Li, X., Gu, D., Qi, J., Ukita, M. & Zhao, H. 2003 Modeling of residual chlorine in water distribution system. *Journal of Environmental Science (China)* **15**, 136–144.

MacCormack, R. W. 2003 The effects of viscosity in hypervelocity impact cratering. *Journal of Spacecraft and Rockets* **40**, 757–763.

Menaia, J., Coelho, S. T., Lopes, A., Fonte, E. & Palma, J. 2002 Dependency of bulk chlorine decay rates on flow velocity in water distribution networks. In: *World Water Congress 2002*, Melbourne, 7–12 April.

Meng, F., Liu, S., Ostfeld, A., Chen, C. & Burchard-Levine, A. 2013 A deterministic approach for optimization of booster disinfection placement and operation for a water distribution system in Beijing. *Journal of Hydroinformatics* **15**, 1042–1058.

Mohapatra, S., Sargaonkar, A. & Labhasetwar, P. K. 2014 Distribution network assessment using EPANET for intermittent and continuous water supply. *Water Resources Management* **28**, 3745–3759.

Percival, S. L., Walker, J. T. & Hunter, P. R. 2000 *Microbiological Aspects of Biofilms and Drinking Water*. CRC Press, Boca Raton, FL.

Pezzinga, G. & Cannizzaro, D. 2014 Analysis of transient vaporous cavitation in pipes by a distributed 2D model. *Journal of Hydraulic Engineering* **140**, 04014019-1–04014019-10.

Powell, J. C. 1998 Modelling Chlorine in Water Distribution Networks. PhD thesis, University of Birmingham, UK.

Qualls, R. G. & Johnson, J. D. 1983 Kinetics of the short-tem consumption of chlorine by fulvic acid. *Environmental Science & Technology* **17**, 692–698.

Ramos, H., Loureiro, D., Lopes, A., Fernandes, C., Covas, D., Reis, L. F. & Cunha, M. C. 2010 Evaluation of chlorine decay in drinking water systems for different flow conditions: from theory to practice. *Water Resource Management* **24**, 815–834.

Rezaei, H., Bryan, B. & Stoianov, I. 2015 Pipe failure analysis and impact of dynamic hydraulic conditions in water supply networks. *Procedia of Engineering* **119**, 253–262.

Shamloo, H. & Mousavifard, M. 2015 Turbulence behavior investigation in transient flows. *Journal of Hydraulic Research* **53**, 83–92.

Termini, D. & Viviani, G. 2015 Spatial diversity of chlorine residual in a drinking water distribution system: application of an integrated fuzzy logic technique. *Journal of Hydroinformatics* **17**, 293–306.

Vieira, P., Coelho, S. T. & Loureiro, D. 2004 Accounting for the influence of initial chlorine concentration, TOC, iron and temperature when modelling chlorine decay in water supply. *Journal of Water Supply: Research and Technology-AQUA* **53**, 453–467.

Warton, B., Heitz, A., Joll, C. & Kagi, R. 2006 A new method for calculation of the chlorine demand in natural and treated waters. *Water Research* **40**, 2877–2884.

Zhao, M. & Ghidaoui, S. 2003 Efficient quasi-two-dimensional model for water hammer problems. *Journal of Hydraulic Engineering* **129**, 1007–1013.

First received 23 July 2016; accepted in revised form 5 January 2017. Available online 8 March 2017